 doi:10.20944/preprints202210.0220.v1

Article

Multi-omic Profiling, Structural Characterization and Potent Inhibitor Screening of Evasion Related Proteins of a Parasitic Nematode, *Haemonchus contortus*, Surviving Vaccine Treatment

Nikola Palevich*, Paul H. Maclean, Vincenzo Carbone, Ruy Jauregui and Saleh Umair

AgResearch Ltd., Grasslands Research Centre, Palmerston North, 4442, New Zealand.
* Correspondence: nik.palevich@agresearch.co.nz

Abstract: The emergence of drug-resistant parasitic nematodes of both humans and livestock calls for development of alternative and cost-effective control strategies. For the economically important ruminant strongylid *Haemonchus contortus*, Barbervax® remains the only registered vaccine available. Here we compared the microbiome, genome-wide diversity and transcriptome of *H. contortus* adult male populations that survived vaccination with an experimental vaccine after inoculation in sheep. Our genome-wide SNP analysis revealed 16 putative candidate vaccine evasion genes. However, we did not identify any evidence for changes in microbial community profiling based of 16S rRNA gene sequencing results of vaccine surviving parasite populations. A total of 58 genes were identified as significantly differentially expressed with six being long non-coding (lnc) RNAs and no putative candidate SNP associated genes. The genes highly upregulated in surviving parasites from vaccinated animals were associated with GO terms belonging to predominantly molecular function and a few biological processes that may have facilitated evasion or potentially lessened the effect of the vaccine. These included five targets: astacin (ASTL), carbonate dehydratase (CA2), phospholipase A2 (PLA2), glutamine synthetase (GLUL) and fatty acid-binding protein (FABP3). We searched all five DEG targets against the proteomes of selected Nematoda (Clades III, V, IV, C, I) and Platyhelminthes (Clades Monogenea, Trematoda, Cestoda, Rhabditophora) to determine homologs within the *H. contortus* NZ_HCO_NP v1.0 genome and identified single-copy orthologous groups (OGs) in selected proteomes. All but one (FABP3) demonstrated high levels of duplication and wide-spread occurrence in closely related *Caenorhabditis elegans* and *Pristionchus pacificus*, with complete absence of all five gene targets among other Clade III (*Toxocara canis*) and V (*Ascaris suum*, *Ascaris lumbricoides* and *Parascaris univalens*) nematodes, further supporting their vital biological functions in nematodes. Phylogenetic analyses inferred the presence of only ASTL and CA2 in almost all Nematoda, platyhelminthes and metazoans examined, with loss of GLULs observed among all outgroup vertebrate species and the presence of FABP3 in only three other species (*Schmidtea mediterranea*, *Fasciola gigantica* and *F. hepatica*). Our tertiary structure predictions and modelling analyses were used to perform *in silico* searches of all published and commercially available inhibitor molecules or substrate analogues with potential broad-spectrum efficacy against nematodes of human and veterinary importance.

Keywords: *Haemonchus contortus*; nematode; genome; transcriptome; microbiome; host-parasite interactions; vaccine

Preprints (www.preprints.org) | NOT PEER-REVIEWED | Posted: 17 October 2022 doi:10.20944/preprints202210.0220.v1

1. Introduction

Haemonchus contortus is a blood-sucking nematode parasite browser and resides in the abomasa of the ruminants. The parasite has a direct life-cycle where the eggs laid by the adult worms are passed on to the pasture through feces (Figure 1A). Eggs develop into the infective stage larvae (L3), which are ingested and reside in the abomasa of the ruminants and develop into adult worms [1]. Parasitic nematode worm infection is one of the biggest health problems for farmed ruminants worldwide [2]. Parasitic worm infections are harmful to a host animal for many reasons and cause costly production losses and if left untreated, animals can die causing further economic loss to farmers.

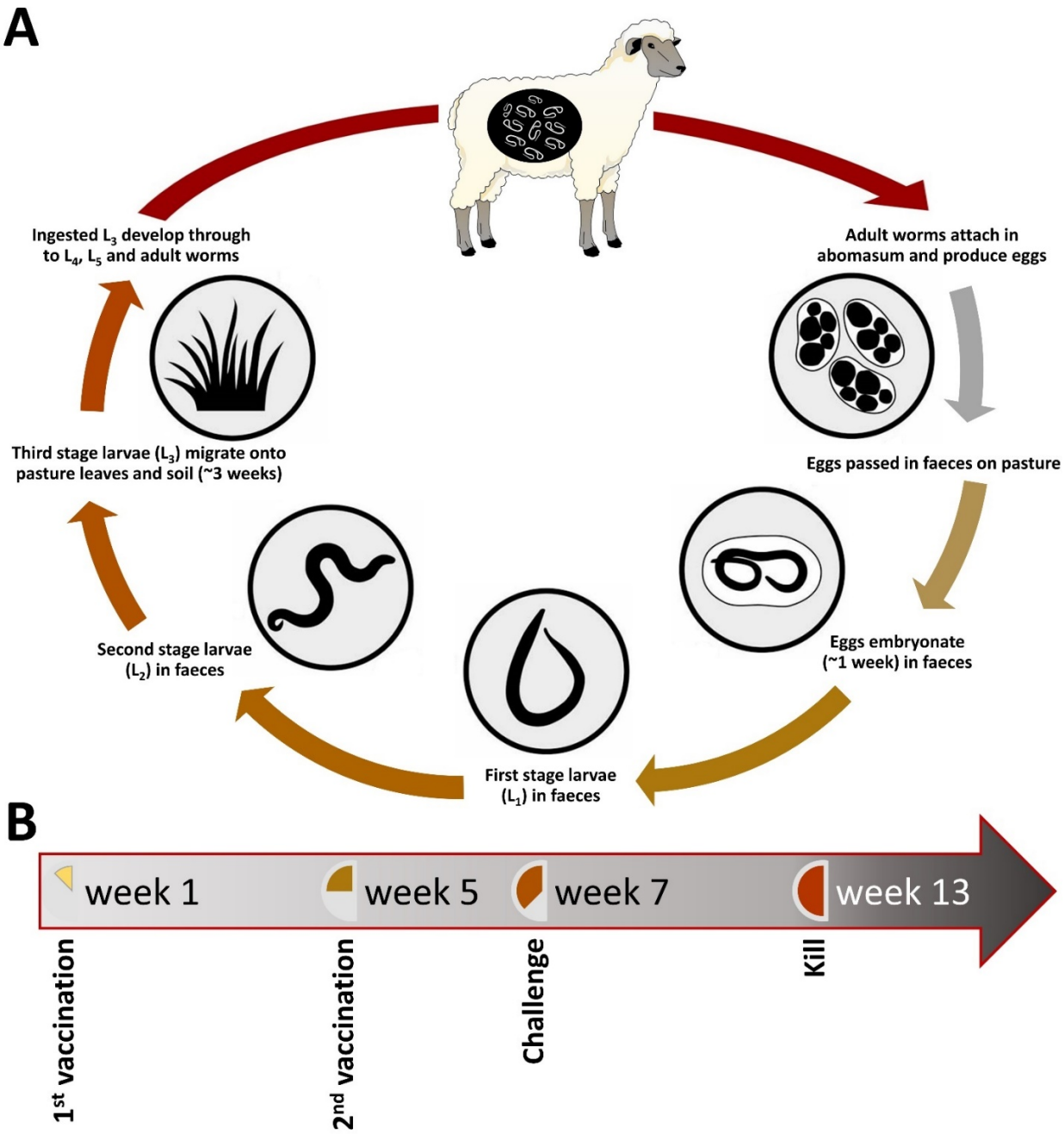

Figure 1. Developmental life cycle of *Haemonchus contortus* parasite in sheep (**A**) and experimental design for parasite sample collection (**B**). Figure adapted from Palevich, et al. [3].

The control and productivity losses caused by parasitic nematodes cost the New Zealand livestock industry ~$700 million annually. Currently, farmers rely on the use of

 doi:10.20944/preprints202210.0220.v1

anthelmintics to control parasitic nematodes, however resistance of parasites to one or more of these agents is now widespread. Recent industry-funded surveys in New Zealand found that 64% of sheep farms and 94% of beef farms now have parasites that are resistant to at least one of the anthelmintics [2].

Alternative methods of controlling the effect of on-farm parasite infections have been proposed and includes altered grazing management, use of nematode trapping fungi, dietary supplements, selective breeding of animals for host resistance and vaccines. Vaccines against parasites can work best by complementing the current drug-based control strategies, and by reducing the frequency of drug use ultimately delay the onset of drug resistance [4]. It is assumed that antibodies, salivary in particular, should be able to reach and target the worms. Attempts to develop vaccines against parasitic nematodes have met with limited success in the past and to date there are very few commercial recombinant vaccines available for any nematode parasites. A vaccine (Barbervax®) based on an extract of adult *H. contortus* has recently been commercialized in Australia [5]. Our recent work aimed aimed at developing a recombinant *Haemonchus* vaccine comprising of 11 antigens has proven effective in weaned lambs as well as the closely related *Teladorsagia circumcincta* vaccine [6-9], however further details around the vaccine composition and efficacy cannot be released.

The recombinant *Haemonchus* vaccine, like every other vaccine, does not provide 100% protection and few adult parasites survive within the vaccinated animals [10-12], then go onto lay eggs, which are passed through animal feces onto the field. High survival rates after treatments, if the treatment has been applied correctly, typically leads to the rapid development of resistance. GIN parasites are well known to avoid its hosts defense mechanisms, but the exact process how it does this is unknown. The high level of genetic diversity observed in GIN combined with their capacity for rapid adaptation are the main contributing factors to the high incidence and evolution of drug resistance. A vaccine can face a similar issue of resistance/ lack of efficacy. Therefore, it is important to understand the mechanism of worm survival against the vaccine. In the present study, we explore the genetic diversity observed in the NZ *H. contortus* genome [13, 14] by investigation of the genomic DNA, microbiome [15] and transcriptomes of adult male *H. contortus* populations obtained from vaccinated and non-vaccinated animals. To gain further insight into the substrate specificities of the genes deemed important for vaccine evasion in *H. contortus*, we selected five significantly differentially expressed genes among adult male worms that survived vaccine treatment and inferred the size of their homologous families within available helminth genomes. This subset of genes were then modelled to determine their tertiary structures using the full-length amino acid sequences and searched for available inhibitor molecules that could be utilized in conjunction with the vaccine.

 doi:10.20944/preprints202210.0220.v1

2. Results and Discussion

2.1. Genome-Wide SNP Analysis Reveals Putative Candidate Vaccine Evasion Genes

H. contortus (barber's pole worm), is one of the most economically important gastrointestinal pathogenic nematodes infecting small ruminants and is a global animal health issue causing drastic losses in livestock [16, 17]. For this study, the recovered *H. contortus* isolate specimens were identified as adult male based on their morphological characteristics [18, 19], and confirmed by PCR assay using *H. contortus*-specific primers [20, 21].

To investigate genetic regions associated with vaccine evasion, the *H. contortus* vaccine treated (n=10) and control (n=9) groups (10 worms per sample) were pooled and WGS was performed on the two populations. The total numbers of trimmed WGS reads in the vaccine treated group was 299,616,531 (raw reads of 345,817,470) compared to 294,245,984 (raw reads of 337,177,268) for the control group. Our genome-wide differentiation scan identified a total of 16,864,411 SNP variants from the filtered WGS data, with 859,860 SNPs that had differing genotypes between the two populations with a genome-wide distribution of 1 SNP per 541 bp on average (Figure 2). Among these only a proportion of the filtered SNPs were associated with just a few but clear genomic regions that differ between the two treatment groups.

Further interrogation of these regions identified a total of 16 putative candidate genes found to be associated with these highly variable regions (Table 1), with almost half of these annotated as hypothetical proteins or proteins of unknown function [22]. Interestingly, a single long non-coding RNA (linc-LOC47095) was identified on chromosome five, but no significant SNP regions were found for either chromosome three or within the mitochondrial genome of *H. contortus* NZ_HCO_NP [14, 23, 24]. Of the candidate genes with putative annotations assigned, the following loci on chromosomes 1, 4, and 5 and associated molecular gene ontology term functions were significantly associated at the genome level: ubiquitin conjugation pathway (NZ_Hco_NP_LOC1281), transcription initiation factor (NZ_Hco_NP_LOC10131), chloride ion channel (NZ_Hco_NP_LOC38016), fatty acid biosynthesis/metabolism, (NZ_Hco_NP_LOC42898), G protein-coupled receptor signaling pathway (NZ_Hco_NP_LOC47058), transcription regulation (NZ_Hco_NP_LOC51467), aminopeptidase (NZ_Hco_NP_LOC55800) and tyrosine-protein kinase (NZ_Hco_NP_LOC54360). The most significant and overrepresented SNP in the vaccinated group corresponds to a locus on chromosome 1 within the gene encoding a putative integrase core domain protein (NZ_Hco_NP_LOC5395), however further bioinformatic resolution and investigation is required to improve its annotation. This preliminary study provides initial support for future investigations targeting the various neuronal signaling and transcription regulation pathways driving the immune mechanisms of vaccine evasion in *H. contortus* and other parasitic nematodes. However, considering the study design, additional work either through increased sample size, additional parasite species or other populations of sheep breed, are needed to validate our preliminary findings.

Preprints (www.preprints.org) | NOT PEER-REVIEWED | Posted: 17 October 2022 doi:10.20944/preprints202210.0220.v1

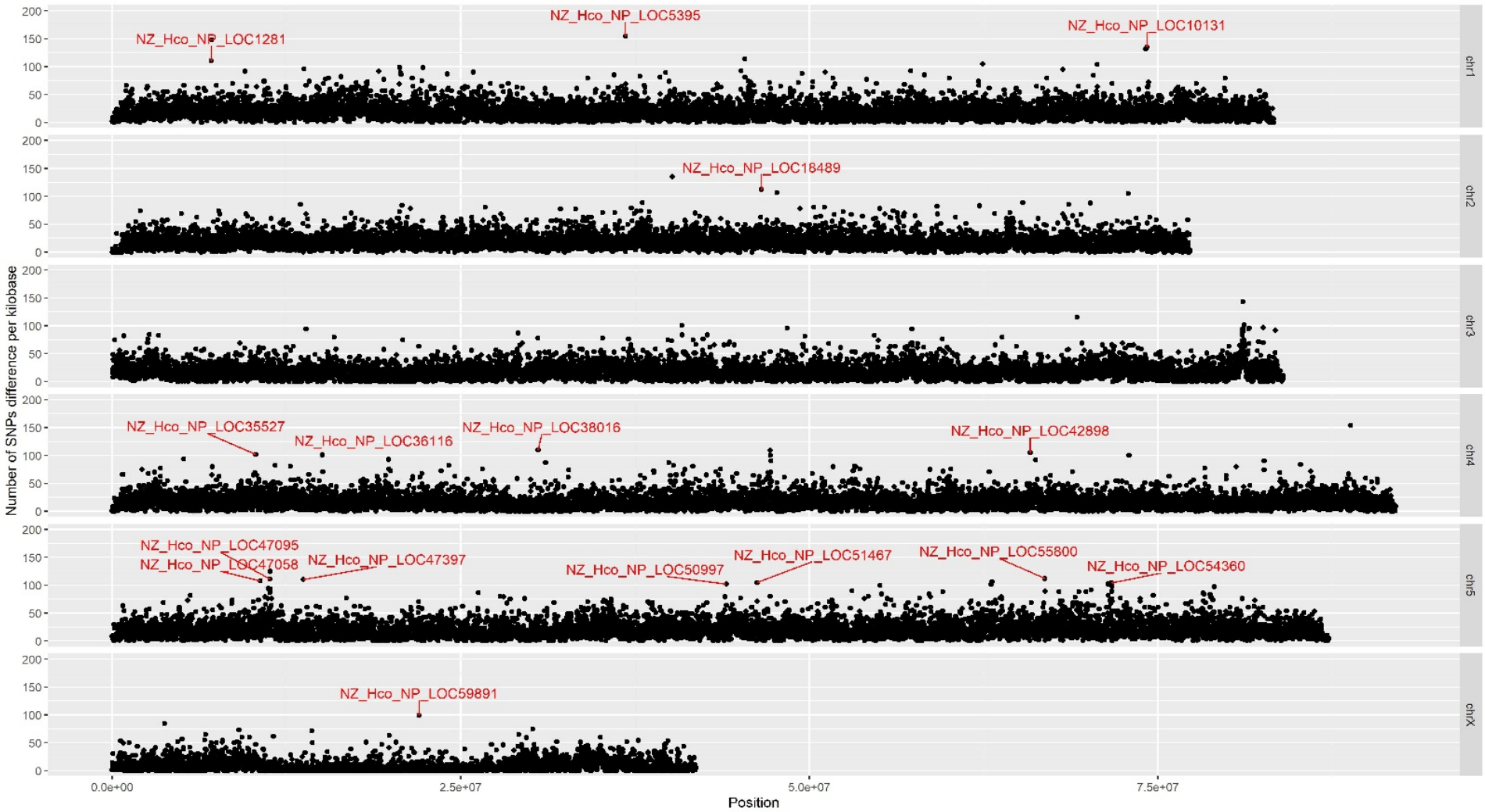

Figure 2. Chromosome-wide distribution of significant SNPs identified with different calls between vaccine treatment and non-treated groups. Chromosomes (chr) 1-5 and X are shown top to bottom with locus tags displayed where significant SNPs are associated with annotated genes over a 10-Kbp window.

 doi:10.20944/preprints202210.0220.v1

2.2. Nematode Microbiome Population Structure Associated with Vaccine Evasion

Microbial community profiling using next-generation sequencing of 16S rRNA gene (V3-V4 region) results showed small but clear changes to the bacterial communities between the control and vaccine treatment groups at both the genus and species levels (Figure 3). Overall, there was no detectable contamination in the majority of the *H. contortus* microbiome samples and the vaccine treatment had small, but significant impacts on the composition of the parasite microbiota. Exceptions to these findings include samples 3 and 19 that were removed from downstream analysis as their profiles were completely different from all other samples (Figure S1). The observed bacterial contamination of the DNA samples was likely due to environmental contaminants that possibly calls for improvements to the current and standard sterilization methods used [25].

A total of eleven different phyla were identified in the adult male *H. contortus* microbiome which were predominantly dominated by bacterial phyla: *Firmicutes* (60%), *Proteobacteria* (36%) and *Bacteroidetes* (3%) (Figure 3A). The predominant genera in the adult male *H. contortus* microbiome was dominated by *Carnobacterium* (32%), *Serratia* (28%), *Lactococcus* (10%), *Streptococcus* (8%) and *Lactobacillus* (4%) (Figure 3B). Samples were evaluated for microbial diversity within samples (alpha diversity) and community diversity between samples (beta diversity) analysis. The Principal Coordinates Analyses (PCoA) of beta diversity using Bray-Curtis dissimilarity results indicated that adult male *H. contortus* (p-value < 0.05) microbiomes clustered together and showed no significant clustering of treated and control samples at the phylum-level (Figure 3C). Alpha diversity measured using Chao1 species richness was lower in the *H. contortus* (p-value < 0.05) vaccine treated group at the phylum-level (Figure 3D), but were similar in terms of species richness (Figure 3E). The biological implications of these findings warrant further validation in future studies by investigating correlations with pre- and post-infection abomasal and faecal microbiomes of the host animal. Overall, the average OTU abundances at phylum-level between the vaccinated and control group microbiome profiles were comparable (Figure 3F), with the only significantly higher bacterial OTU abundance observed among *Tenericutes* for the control group.

Animal studies of helminthiases can offer a comprehensive snapshot of the diverse influences that nematodes have on the gut microbiota of their hosts and account for the limitations associated with sampling only the fecal microbiota [26]. In the absence of external contaminants of the parasites, the adult male *H. contortus* microbiomes were characterized by *Serratia*, *Citrobacter*, *Pseudomonas*, *Aeromonas*, *Prevotella*, and *Shigella* were identified among gram-negatives while *Carnobacterium*, *Lactococcus*, *Streptococcus*, *Lactobacillus*, *Vagococcus* and *Enterococcus* were identified amongst gram-positive organisms. These results are similar to those observed in earlier studies conducted on *H. contortus* microbiomes, that reported overall bacterial phyla dominatation by: *Firmicutes* followed by *Proteobacteria* and *Bacteroidetes* [15, 25, 27, 28].

 doi:10.20944/preprints202210.0220.v1

Table 1. Genome-wide SNP analysis using whole-genome sequencing of adult male *H. contortus* identifies candidate genes putatively associated with vaccine evasion.

SNP ID	Chromosome	Position (bp)	SNP per KB	Fisher's *P-Value*	Locus Tag	Gene Description
NZ_Hco_NP_LOC1281	chr 1	7,110,000	148	1.80E-41	NZ_Hco_NP_LOC1281	Zinc finger in N-recognin
NZ_Hco_NP_LOC5395	chr 1	36,800,000	155	1.62E-45	NZ_Hco_NP_LOC5395	Putative integrase core domain protein
NZ_Hco_NP_LOC10131	chr 1	74,220,000	135	2.71E-34	NZ_Hco_NP_LOC10131	Transcription initiation factor IIA, helical domain protein
NZ_Hco_NP_LOC18489	chr 2	46,570,000	112	8.60E-23	NZ_Hco_NP_LOC18489	Unknown
NZ_Hco_NP_LOC35527	chr 4	10,300,000	102	2.45E-18	NZ_Hco_NP_LOC35527	Hypothetical protein
NZ_Hco_NP_LOC36116	chr 4	15,080,000	101	6.53E-18	NZ_Hco_NP_LOC36116	Unknown
NZ_Hco_NP_LOC38016	chr 4	30,550,000	110	7.14E-22	NZ_Hco_NP_LOC38016	Bestrophin-1 domain protein
NZ_Hco_NP_LOC42898	chr 4	65,840,000	105	1.23E-19	NZ_Hco_NP_LOC42898	GNS1/SUR4 family protein
NZ_Hco_NP_LOC47058	chr 5	10,610,000	108	5.75E-21	NZ_Hco_NP_LOC47058	G_PROTEIN_RECEP_F1_2 domain-containing protein
NZ_Hco_NP_LOC47095	chr 5	11,310,000	111	2.49E-22	NZ_Hco_NP_LOC47095	Long non-coding RNA lnc-LOC47095
NZ_Hco_NP_LOC47397	chr 5	13,700,000	110	7.14E-22	NZ_Hco_NP_LOC47397	Unknown
NZ_Hco_NP_LOC50997	chr 5	44,040,000	102	2.45E-18	NZ_Hco_NP_LOC50997	Hypothetical protein
NZ_Hco_NP_LOC51467	chr 5	46,260,000	105	1.23E-19	NZ_Hco_NP_LOC51467	Ligand-binding domain of nuclear hormone receptor
NZ_Hco_NP_LOC55800	chr 5	66,890,000	112	8.60E-23	NZ_Hco_NP_LOC55800	Peptidase M1 domain containing protein
NZ_Hco_NP_LOC54360	chr 5	71,650,000	104	3.37E-19	NZ_Hco_NP_LOC54360	Protein tyrosine kinase
NZ_Hco_NP_LOC59891	chr X	22,000,000	99	5.56E-17	NZ_Hco_NP_LOC59891	Hypothetical protein

Preprints (www.preprints.org) | NOT PEER-REVIEWED | Posted: 17 October 2022 doi:10.20944/preprints202210.0220.v1

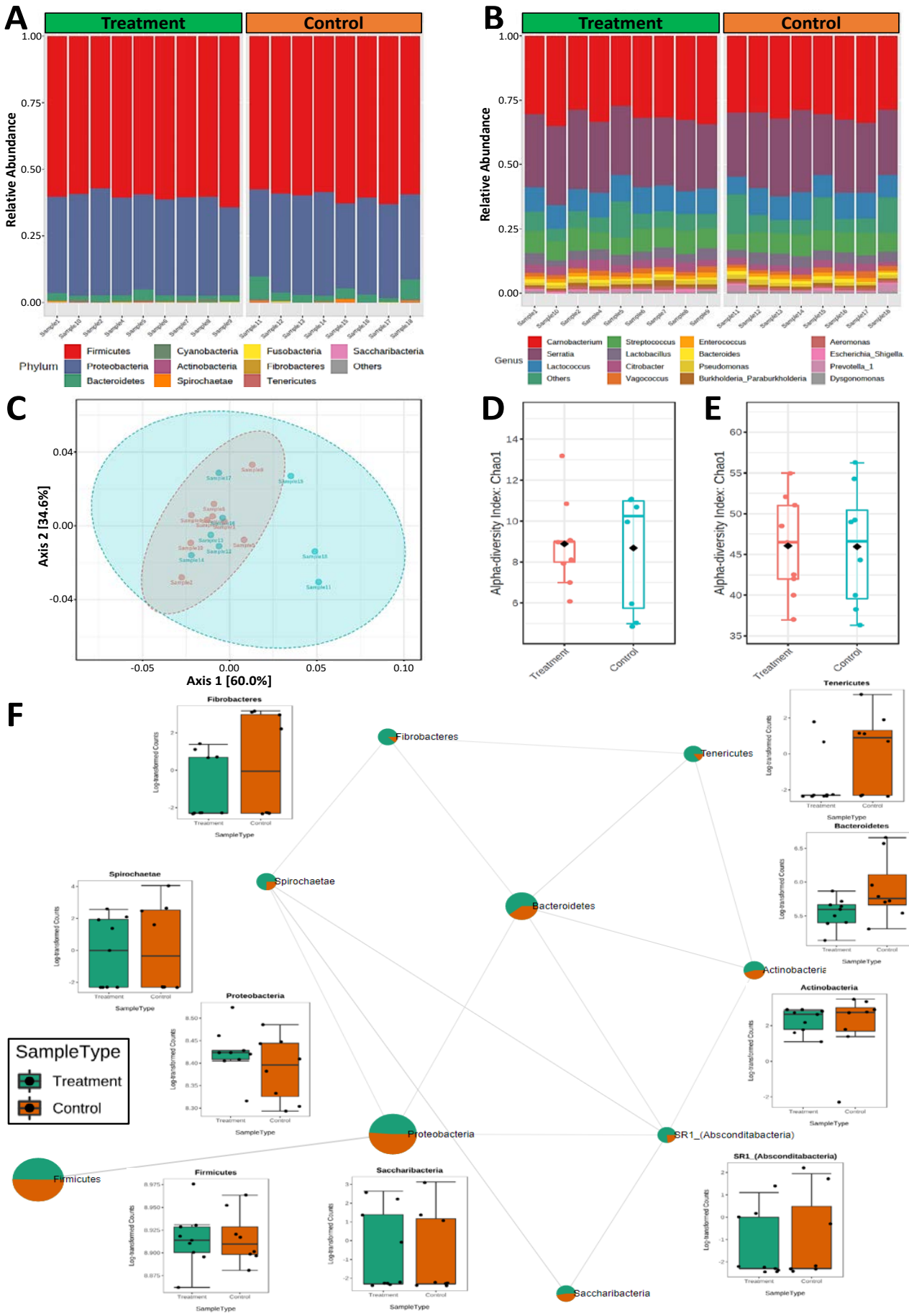

Preprints (www.preprints.org) | NOT PEER-REVIEWED | Posted: 17 October 2022 doi:10.20944/preprints202210.0220.v1

Figure 3. Microbial composition and profiling of adult male nematodes from vaccine treated and control animals. Each sample is derived from a pooled mixture of ten adult male nematodes taken from the ovine abomasum at postmortem. Phyla constituting less than 1% of the total phylum distribution for a sample were labelled 'Others'. Top ten phyla (**A**) and fifteen genera (**B**) level features correlated with control or vaccine treated groups. (**C**) Phylum-level Bray-Curtis dissimilarity correlations of the treatment (red) and control (blue) nematode microbiomes. Alpha diversity boxplots showing Chao1 species richness determined using the Mann-Whitney U test at phylum (**D**) and genus (**E**) level of treatment (red) and control (blue) microbiomes. Co-abundance groups interaction network based on relative abundance of bacterial phyla in nematodes from vaccinated (green) and non-treated control (orange) animals (**F**). Node size represents the average abundance of each OTU with lines between nodes representing correlations to each other. The corresponding boxplots show log-transformed counts for each phyla. In each plot, the box represents the interquartile range, the line inside the box represents the median and whiskers denote the minimum and maximum values.

Although the reported *H. contortus* samples were recovered from sheep of the same breed, diet and environmental conditions, variations in the microbiomes between adult male and female *H. contortus* may occur in response to vaccine exposure.These sex-specific alterations can be associated with host immunity or in response to hormone production and egg development in females. However, further information can be provided by investigating the different parasite life-cycle stages and adult female *H. contortus* microbiomes in future investigations. The common microbiome profiles of both vaccine treated and control group *H. contortus* adult males suggest that the worm microbiome has a potentially important nutritional role in the breakdown of the blood meal or endogenous supply of growth promoting metabolites that the worm cannot produce itself.

2.3. Transcriptional Changes and Differential Gene Expression

We investigated changes in gene expression of *H. contortus* adult male worms from vaccinated relative to non-vaccinated control sheep. The total numbers of the trimmed reads in vaccine treated group was 1,139,856,121 (raw reads of 1,166,781,856) compared to 735,099,192 (raw reads of 753,304,040) for the control group (Figure S1A-B). PCA is a dimensionality reduction method that makes use of transcript counts to define a new set of unrelated components. Coordinates of every pool of worms considered for analysis are plotted against the first two components and correlate with similarities between pools. In our PCA analysis of the normalized RNA-seq read counts, the first PCA axis explains 66% of total variance and relates to differences between the vaccinated and control experimental groups (Figure S1C). Two samples representing pools of worms sampled from control sheep (RNA_2 and RNA_18) were discarded from the dataset for subsequent analyses based on their abnormal transcriptomes.

The RNA-Seq reads were mapped to the *H. contortus* NZ_HCO_NP [14, 23, 24] genome and genes with copies less than 1 copy per million (CPM) in all the samples were filtered out, resulting in 45,794 unique genes (of which 24,717 putatively encoded proteins) identified and normalized for differential expression analysis. A total of 601 differentially expressed genes (DEGs) were identified that had false discovery rate (FDR) adjusted P value < 0.05 (above horizontal dashed red line, Figure S1D), and absolute high/low fold change > 1.5 (outside vertical dashed red lines, Figure S1E). Once the stringent cutoff thresholds were applied (logCPM >200, $\log_2$FC >2, adjusted P value <0.01), 58 genes were identified as significant DEGs between the two experimental groups (Tables S2). All of the significant DEGs were upregulated with the majority located on chromosomes four and X, with only the gene encoding an RNA recognition motif domain containing protein (NZ_Hco_NP_LOC34257) found on chromosome three (Table 2). Among the significant DEGs, a total of eight genes were annotated as hypothetical proteins or proteins of unknown function (Table S2). Multiple copies of genes encoding chitin binding peritrophin-A domain proteins (NZ_Hco_NP_LOC61624, NZ_Hco_NP_LOC61553, NZ_Hco_NP_LOC2894, NZ_Hco_NP_LOC5035); fibrous sheath CABYR-binding protein (NZ_Hco_NP_LOC56212); low density lipoprotein-receptor protein (NZ_Hco_NP_LOC24365); chondroitin proteoglycan 4 domain-containing protein (NZ_Hco_NP_LOC44247) and zinc finger domain containing protein (NZ_Hco_NP_LOC9950). Also, four DEGs had directly co-located significant DEGs

 doi:10.20944/preprints202210.0220.v1

encoding hexokinase domain containing protein (NZ_Hco_NP_LOC4700-1), peptidase A1 domain containing protein (NZ_Hco_NP_LOC35463-4), peptidase M1 domain containing protein (NZ_Hco_NP_LOC54152-4) and phospholipase A2 (NZ_Hco_NP_LOC13325-6).

Notably, none of the putative candidate SNP associated genes from our genome-wide analysis were found to be significantly differentially expressed (Table 2). However, SNPs associated with the gene encoding a GNS1/SUR4 family protein (NZ_Hco_NP_LOC42898) was found to be the most differentially expressed from our datasets. Members of this gene family (Pfam01151) have numerous homologues in *C. elegans* and are predicted to be integral membrane proteins involved in long chain fatty acid elongation systems [29] and act on glucose-signaling pathways by modulating plasma membrane H^+-ATPase activity [30]. In addition, six long non-coding (lnc) RNAs (NZ_Hco_NP_LOC12416, NZ_Hco_NP_LOC39485, NZ_Hco_NP_LOC61876, NZ_Hco_NP_LOC61506, NZ_Hco_NP_LOC56711, NZ_Hco_NP_LOC14268) were significantly differentially expressed (Table S2). lncRNAs perform vital functions by interacting with mRNA, DNA, protein, and miRNA to consequently regulate gene expression at the epigenetic, transcriptional, post-transcriptional, translational, and post-translational levels in a variety of ways to regulate responses to environmental stresses in organisms [31-33]. While very little is known about the roles of lncRNAs and the regulatory pathways affected within parasitic nematodes, our findings encourage future exploratory studies of different nematode tissues or investigations using multicellular *in vitro* culture systems such as organoids [34] to better understand the roles of lncRNAs.

Preprints (www.preprints.org) | NOT PEER-REVIEWED | Posted: 17 October 2022 doi:10.20944/preprints202210.0220.v1

Table 2. Genome-wide SNP analysis using whole-genome sequencing of adult male *H. contortus* identifies candidate genes putatively associated with vaccine evasion.

	Locus Tag	Chromosome	Gene Description	logCPM[a]	FC	logFC[b]	adj. *P*[c]
Top Differentially Expressed (DE)	NZ_Hco_NP_LOC4701	chr 1	Hexokinase domain containing protein	374.11	13.64	3.77	4.47E-72
	NZ_Hco_NP_LOC8487	chr 1	Carbonate dehydratase, eukaryotic-type	273.67	221.36	7.79	4.06E-49
	NZ_Hco_NP_LOC6491	chr 1	Transporter, major facilitator family protein	299.39	4.34	2.12	4.71E-34
	NZ_Hco_NP_LOC10216	chr 1	Patched family protein	202.18	6.14	2.62	9.13E-23
	NZ_Hco_NP_LOC13594	chr 2	Peptidase S1/S6 domain containing protein	379.72	24.66	4.62	6.14E-71
	NZ_Hco_NP_LOC12468	chr 2	Zinc finger domain containing protein	938.69	9.67	3.27	1.68E-56
	NZ_Hco_NP_LOC19286	chr 2	Multifunctional protein ADE2, SAICAR synthetase	228.43	35.58	5.15	1.11E-37
	NZ_Hco_NP_LOC13325	chr 2	Phospholipase A2	1,553.99	14.60	3.87	1.02E-09
	NZ_Hco_NP_LOC34257	chr 3	RNA recognition motif domain containing protein	650.65	6.43	2.68	6.01E-44
	NZ_Hco_NP_LOC36485	chr 4	PERMeable eggshell protein PERM-2	1,045.16	11.97	3.58	1.72E-91
	NZ_Hco_NP_LOC34077	chr 4	Glutamine synthetase, beta-grasp domain protein	460.76	12.81	3.68	6.55E-70
	NZ_Hco_NP_LOC44234	chr 4	Chondroitin proteoglycan 4 domain-containing protein	6,439.30	176.79	7.47	1.29E-55
	NZ_Hco_NP_LOC39532	chr 4	Glycosyl hydrolase, family 18	875.07	17.10	4.10	4.44E-50
	NZ_Hco_NP_LOC45198	chr 4	Hsp20/alpha crystallin family protein	3,904.34	300.66	8.23	3.91E-42
	NZ_Hco_NP_LOC39044	chr 4	Phosphoribosylglycinamide formyltransferase	231.50	5.94	2.57	7.83E-42
	NZ_Hco_NP_LOC35958	chr 4	Class II glutamine amidotransferase	1,167.18	5.45	2.45	5.14E-35
	NZ_Hco_NP_LOC35968	chr 4	Glutamine-fructose-6-phosphate transaminase	1,318.78	4.11	2.04	1.42E-32
	NZ_Hco_NP_LOC35463	chr 4	Peptidase A1 domain containing protein	447.74	193.29	7.59	2.55E-18
	NZ_Hco_NP_LOC55104	chr 5	Chondroitin proteoglycan 3	495.52	107.16	6.74	3.99E-106
	NZ_Hco_NP_LOC54152	chr 5	Peptidase M1 domain containing protein	558.27	16.17	4.01	1.17E-57
	NZ_Hco_NP_LOC55927	chr 5	Fibrous sheath CABYR-binding protein	2,197.76	882.98	9.79	1.97E-33
	NZ_Hco_NP_LOC54628	chr 5	Diacylglycerol acyltransferase	240.81	38.96	5.28	3.94E-25
	NZ_Hco_NP_LOC56712	chr X	Low-density lipoprotein receptor domain class A	722.49	81.50	6.35	5.39E-120
	NZ_Hco_NP_LOC56407	chr X	Innexin inx-3	479.37	13.91	3.80	1.67E-74
	NZ_Hco_NP_LOC57394	chr X	Fatty acid-binding protein 3	2,172.79	4.01	2.00	8.00E-57
	NZ_Hco_NP_LOC58311	chr X	Protein-tyrosine phosphatase	319.44	5.54	2.47	3.42E-39
	NZ_Hco_NP_LOC56508	chr X	Lactamase_B domain-containing protein	404.68	4.85	2.28	1.61E-30

 doi:10.20944/preprints202210.0220.v1

	NZ_Hco_NP_LOC61374	chr X	von Willebrand factor type D domain protein	342.28	49.01	5.61	6.94E-28
	NZ_Hco_NP_LOC58549	chr X	Chitin binding Peritrophin-A domain protein	8,763.11	232.54	7.86	1.86E-19
	NZ_Hco_NP_LOC61472	chr X	Astacin	231.32	385.77	8.59	8.97E-18
Top SNP Associated Genes	NZ_Hco_NP_LOC1281	chr 1	Zinc finger in N-recognin	2,052.89	1.02	0.03	8.43E-01
	NZ_Hco_NP_LOC5395	chr 1	Integrase core domain protein	220.55	1.22	0.28	4.36E-01
	NZ_Hco_NP_LOC10131	chr 1	Transcription initiation factor IIA	75.74	1.07	0.09	7.77E-01
	NZ_Hco_NP_LOC18489	chr 2	Unknown	130.46	1.08	0.11	8.61E-01
	NZ_Hco_NP_LOC35527	chr 4	Frag1 DRAM Sfk1 domain containing protein	24.61	1.13	0.17	7.50E-01
	NZ_Hco_NP_LOC36116	chr 4	Unknown	14.07	1.12	0.17	7.82E-01
	NZ_Hco_NP_LOC38016	chr 4	Bestrophin-1 domain protein	29.02	1.10	0.14	8.09E-01
	NZ_Hco_NP_LOC42898	chr 4	GNS1/SUR4 family protein	1,409.99	1.21	0.28	9.66E-03
	NZ_Hco_NP_LOC47058	chr 5	G_PROTEIN_RECEP_F1_2 domain-containing protein	35.29	1.21	0.28	3.49E-01
	NZ_Hco_NP_LOC47095	chr 5	Long non-coding RNA lnc-LOC47095	182.47	1.10	0.13	7.82E-01
	NZ_Hco_NP_LOC47397	chr 5	Unknown	200.62	1.94	0.95	1.21E-02
	NZ_Hco_NP_LOC50997	chr 5	Hypothetical protein	318.21	1.14	0.19	1.74E-01
	NZ_Hco_NP_LOC51467	chr 5	Ligand-binding domain of nuclear hormone receptor	1,293.87	1.03	0.05	8.24E-01
	NZ_Hco_NP_LOC55800	chr 5	Peptidase M1 domain containing protein	18,187.44	1.01	0.02	9.63E-01
	NZ_Hco_NP_LOC54360	chr 5	Protein tyrosine kinase	198.19	1.08	0.11	7.34E-01
	NZ_Hco_NP_LOC59891	chr X	Hypothetical protein	161.38	1.09	0.13	7.36E-01

Fold-change is abbreviated to FC. [a]Normalized counts per million (CPM). [b]log-FC in expression as measured by DeSeq2 accordingly. [c]P values adjusted for multiple testing. Cutoff thresholds applied include: log FC >2 and <-2, FDR <0.01, logCPM >200.

Preprints (www.preprints.org) | NOT PEER-REVIEWED | Posted: 17 October 2022 doi:10.20944/preprints202210.0220.v1

Ontology analysis of the DEGs revealed that 351 (58.4% of the total DEGs) DEGs were significantly upregulated in the vaccine treated group samples and had corresponding hits to GO terms. Our analysis revealed 20 significant GO terms belonging to molecular function and another three GO terms belonging to biological process (Figure 4 and Table S3).

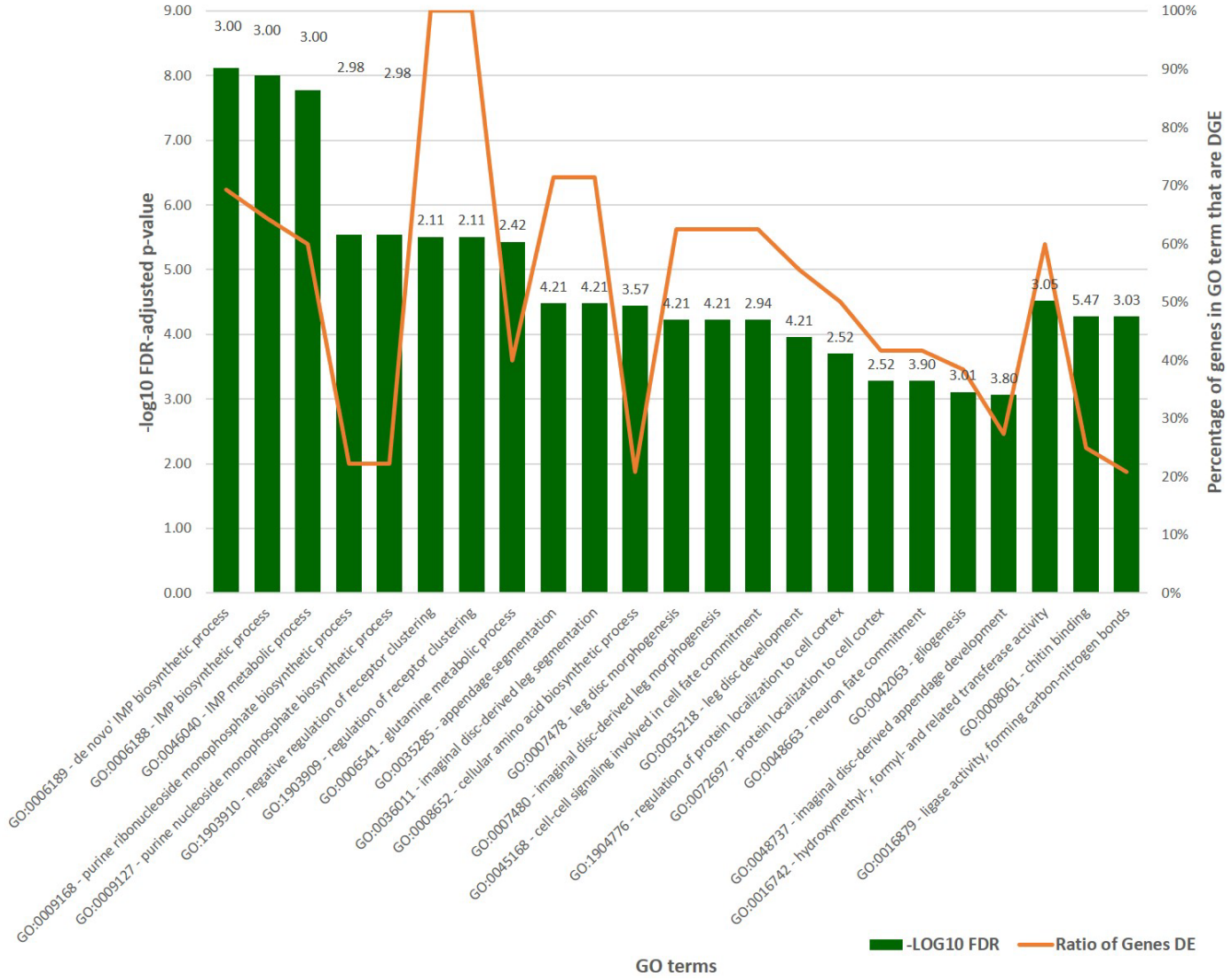

Figure 4. Significant GO terms for differentially expressed genes (DEGs) between vaccinated and non-treated control groups. Mean logFC was measured using DeSeq2 is shown for each GO classification above each bar.

The most significant GO terms affiliated with molecular function (based on -$\log_{10}$FDR) were all related and included de novo' IMP biosynthetic process, IMP biosynthetic process and IMP metabolic process (GO:0006188-40), while the GO terms belonging to biological process included hydroxymethyl-, formyl- and related transferase activity (GO:0016742), chitin binding (GO:0008061) and ligase activity, forming carbon-nitrogen bonds (GO:0016879). The significant GO terms with the greatest number of genes associated were related to purine ribonucleoside and ribonucleoside monophosphate biosynthetic processes (GO:0009168 and GO:0009127). Analysis by fold-change showed that the most enriched cluster of GO terms with subcategories in molecular function included appendage segmentation (GO:0035285), imaginal disc-derived leg segmentation (GO:0036011), leg disc development (GO:0035218) all with mean logFC of 4.21. In addition to the genes encoding chitin binding peritrophin-A domain proteins mentioned above, the most enriched GO term with a mean logFC of 5.47 was associated with chitin binding (GO:0008061) and a total of nine genes. The biological impact of these changes in gene

 doi:10.20944/preprints202210.0220.v1

expression and implications for vaccine evasion within the host animal warrant further investigation.

The high expression and diverse GO term associations of five genes encoding an astacin (ASTL, NZ_Hco_NP_LOC61472, P:GO:0006508 and GO:0018996, F:GO:0004222 and GO:0046872), carbonate dehydratase (CA2, NZ_Hco_NP_LOC8487, F:GO:0004089 and GO:0008270), phospholipase A2 (PLA2, NZ_Hco_NP_LOC13325, P:GO:0006644, GO:0016042 and GO:0050482, F:GO:0004623 and GO:0005509), glutamine synthetase (GLUL, NZ_Hco_NP_LOC34077, P:GO:0006542, F:GO:0004356 and GO:0005524) and fatty acid-binding protein (FABP3, NZ_Hco_NP_LOC57394, F:GO:0008289), was the basis for their selection for further investigation of their evolutionary significance.

2.4. Orthology and Evolution of Significant DEGs

In order to investigate their potential for repurposing of existing therapeutics and whether the putative vaccine-evasion associated DEGs identified for *H. contortus* are shared between other helminths, we performed orthology-directed phylogenetic analyses of *H. contortus* ASTL, CA2, PLA2, GLUL and FABP3 to visualize gene gain and loss among representative helminths (Figure 5). In particular, we searched the complete genomes or transcriptomes and acquired genome-wide coding sequences from 27 species representing clades I-V of nematoda, platyhelminths and free-living flatworms (monogenea, digenea, cestoda), as well as human, mice and zebrafish as outgroups. For this analysis, we used orthologous groups (OGs) of genes identified based on the five selected and significantly differentially expressed genes of interest for *H. contortus* and we modeled gene gain and loss for the five orthologues. Comparative analysis within ASTL (OG0000012), CA2 (OG0000190), PLA2 (OG0000857), GLUL (OG0015501), and FABP3 (OG0003610) revealed several examples of clade-specific conservation of orthology profiles, with no enzyme or protein present across all nematode (Figure 5).

The complete absence or loss of all five OGs investigated was observed for *Toxocara canis* (Clade III) and the Clade V nematodes *Ascaris suum*, *A. lumbricoides* and *Parascaris univalens*. Our phylogenetic analyses indicate that ASTLs and CA2s appear to be broadly conserved across all species compared in our study and are ancient eukaryotic gene families, with the exceptions of the four above-mentioned species and *Gyrodactylus salaris* (ASTL, Monogenea). In contrast, PLA2s and GLULs appear to have been lost independently within eukaryotes, especially in Trematoda and Cestoda lineages, with loss of GLULs also observed for Rhabditophora.

Preprints (www.preprints.org) | NOT PEER-REVIEWED | Posted: 17 October 2022 doi:10.20944/preprints202210.0220.v1

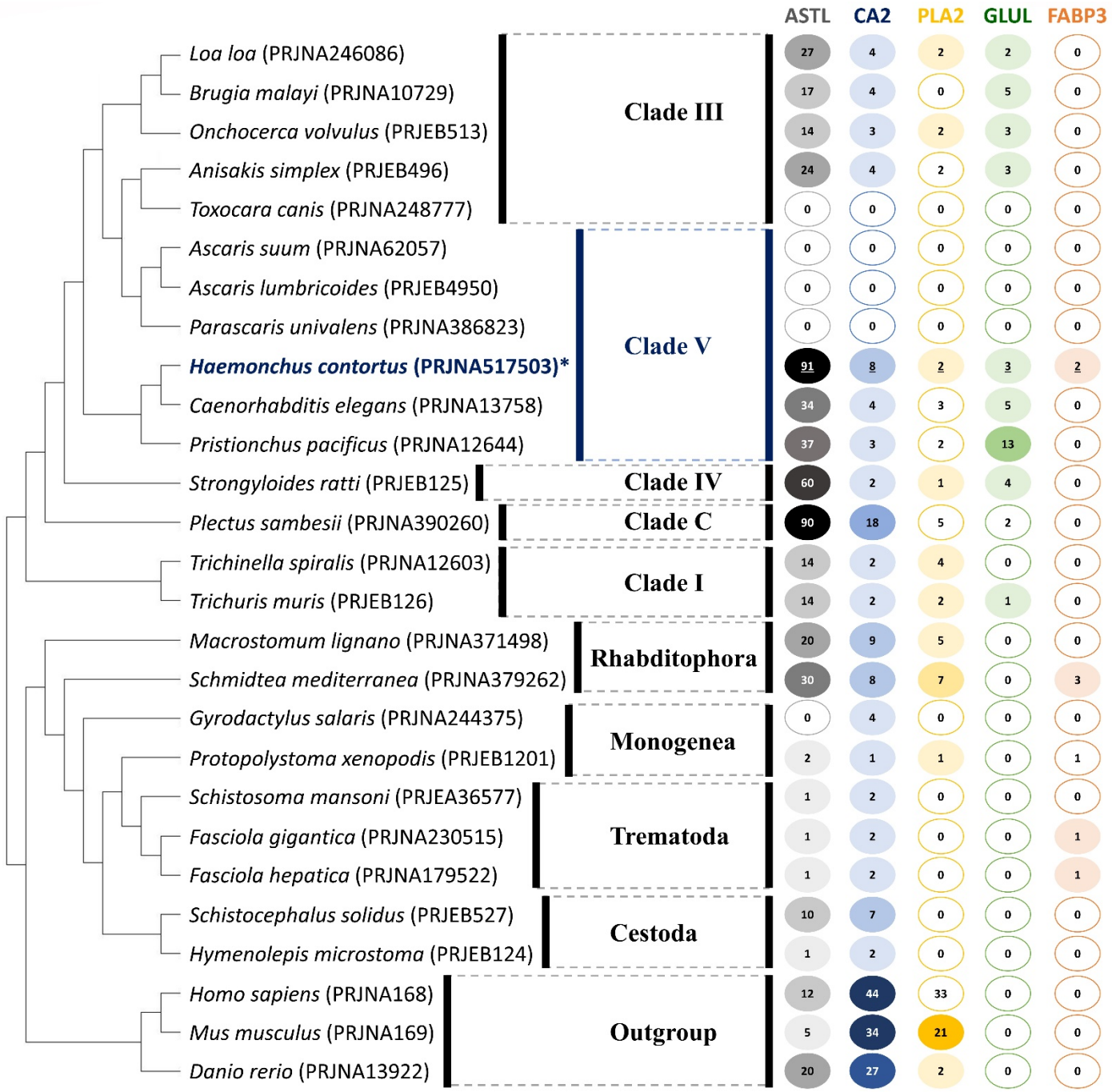

Figure 5. Phylogenetic species-tree reconstruction of homologous gene families corresponding to the five DEGs of interest across 27 species. The consensus tree is based on losses and gains of orthologous groups corresponding to the protein sequence alignments of the five target DEGs of *H. contortus*: ASTL, CA2, PLA2, GLUL and FABP3 (labelled with *). The numbers in colored circles represent the total number of gene families corresponding to a particular gene based on orthology. A missing value indicates the absence of an orthologous group corresponding to any of the five target DEGs of *H. contortus*. Bioproject GenBank accession numbers are provided (in parentheses) for all reference sequences.

 doi:10.20944/preprints202210.0220.v1

Our preliminary orthology analysis of the *H. contortus* ASTLs produced a substantial number of overall homologous sequences (*n*=91 for ABCB9) due to the large and diverse nature of domain architectures of astacin proteins. In particular, the high levels of duplication and wide-spread occurrence of ASTLs and CA2s in closely related Clade V group nematodes (*C. elegans* and *Pristionchus pacificus*), *Strongyloides ratti* (*n*=60, Clade IV) and *Plectus sambesii* (*n*=90, Clade C), implies that these genes may have vital biological functions associated with vaccine evasion. Interestingly, FABP3 orthologues were identified in only *Schmidtea mediterranea* (Rhabditophora) and the Trematodes *Fasciola gigantica* and *F. hepatica*. It is not clear why only these species contain any recognizable FABP3 gene, but leads us to propose that these observations may be due to substantial divergence of FABP3 or the existence of a unique and yet to be characterized pathway for lipid metabolism. Overall, our analysis of the evolutionary significance of the putative vaccine-evasion DEG-associated proteins reflects the specific host-parasite relationships [35], diversity of parasite biology and unique pathogenic strategies formed during their evolution.

2.5. Structures of Selected Immune Evasion-Related Proteins and Potential Drug-Targeting

The five preselected parasite proteins of interest were modeled using the ICM-Pro modelling suite (https://www.molsoft.com/icm_pro.html) to produce tertiary structures of the *Haemonchus* enzymes to elucidate any unique secondary structural motifs and active site compositions (Figure 6 and Table S4). Overall sequence identity remained low (between 28-42 %) for the modelled proteins but when compared to the active site domains, it increases significantly. For the modelled FAB3 protein this was 37.5 % when superimposed with human myelin protein P2 bound to palmitic acid (PDB code 5N4P [36]) with an RMSD of 0.194 Å. The active site is delineated/identified by residues Met165, Tyr148, Tyr56, Val163, Arg174, Phe53, Leu57, Tyr176, Lys97, Glu78, Tyr62, Leu115, Val104, Asp102 and Tyr101. For PA2, the active site identity was 64 % when superimposed by the inhibitor bound human secreted phospholipase A2 protein (PDB code 4UY1 [37]), including residues Pro64, Trp150, Arg52, Leu53, Phe76, Asp94, His93, Gly75, Cys74, Cys90 and an RMSD of 0.874 Å. The catalytic domain depicted in mammalian (human) glutamine synthetase was absent from sequencing and eventual modelling efforts with our differentially expressed parasite protein, however a partial ADP binding site within the Beta-grasp domain of glutamine synthetase was modelled and include identical residues Trp122, Phe124 and Glu126 and an RMSD of 0.133 Å. The metal binding proteins astacin and carbonate dehydratase had near identical zinc binding domains, most likely a conserved motif, between parent structure and model composed of a core of three histidine's and a glutamic acid which help coordinate the single Zn ion. The active site of astacin has a 75 % identity with a zinc metalloprotease from Zebrafish (PDB code 3LQB [38]), bound in a deep cleft between N and C terminals made up in part by conserved residues His224, His228, His234, Glu225 and Tyr283. For carbonate dehydratase, active site residues present within our model and four angstrom of the superimposed human structure bound to ethoxzolamide (EZL) a known carbonic anhydrase inhibitor (PDB code 3MDZ), are 100 % identical and include residues His130, His132, His149, Glu136, Val151, Val170 and an RMSD of 0.226 Å.

Preprints (www.preprints.org) | NOT PEER-REVIEWED | Posted: 17 October 2022 doi:10.20944/preprints202210.0220.v1

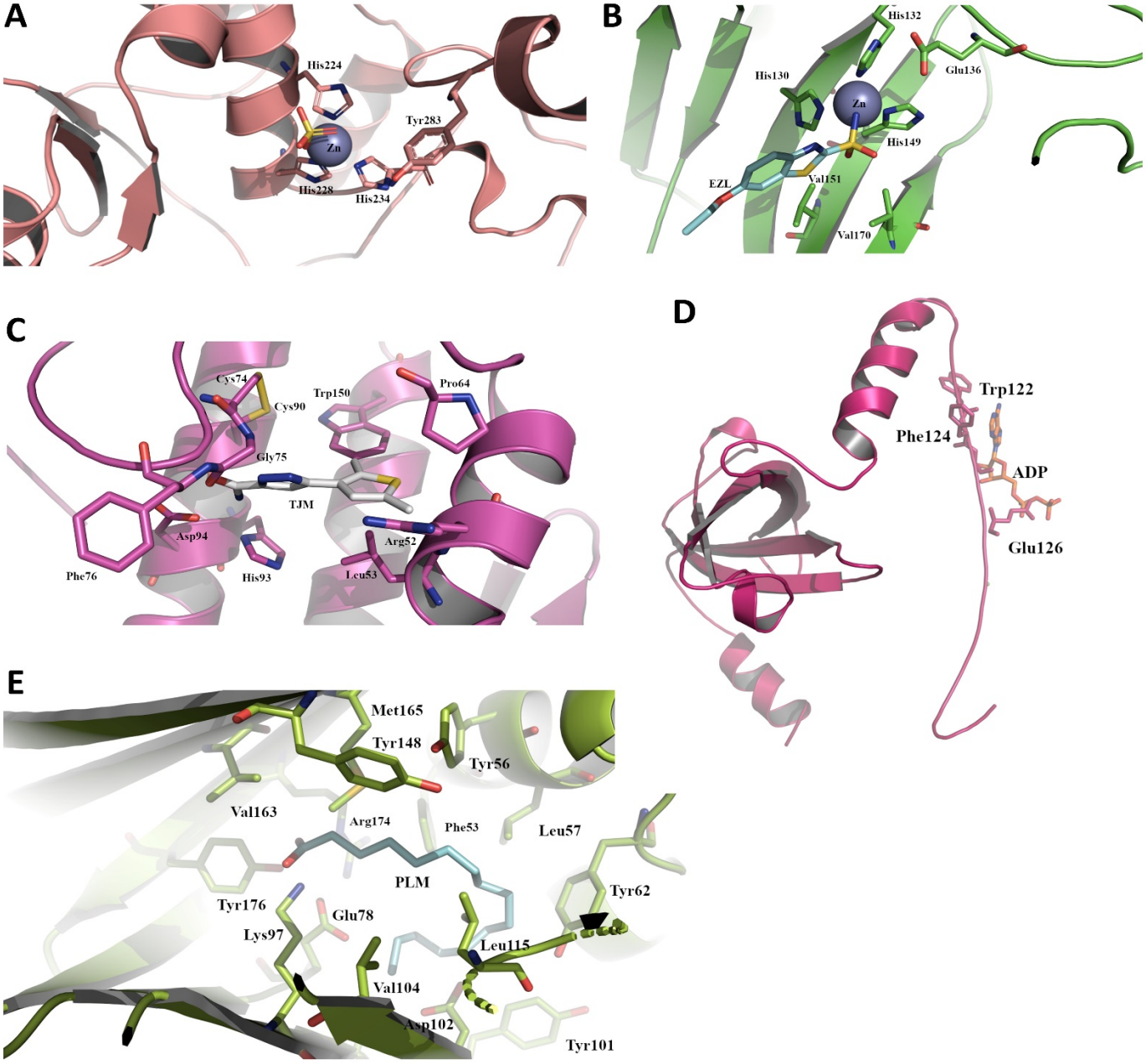

Figure 6. The predicted active site domains of some of the differentially expressed parasite genes including (**A**) Zinc-dependent metalloprotease astacin (ASTL), (**B**) Carbonate dehydratase (CA2), (**C**) Phospholipase A2 (PLA2), (**D**) Glutamine synthetase, Beta-grasp domain protein (GLUL) and (**E**) Fatty acid-binding protein 3 (FABP3). Bound molecules identifying the active site domains were derived from the template structures our models were based on, including the zinc and sulfate molecules in astacin from a zinc metalloprotease from Zebrafish (PDB code 3LQB [38]), Ethoxzolamide (EZL) a known carbonic anhydrase inhibitor and zinc bound to carbonate dehydratse (PDB code 3MDZ), a pyrazole based inhibitor 5-(2,5-dimethyl-3-thienyl)-1h-pyrazole-3-carboxamide (TJM) in the phospholipase model (PDB code 4UY1 [37]), a portion of the ADP binding domain present on the glutamine synthetase, Beta-grasp domain derived from human glutamine synthetase (PDB code 2QC8 [39]) and palmitic acid bound to human myelin protein P2 (PDB code 5N4P [36]). Residues withing 4 Å of the bound and superimposed molecules are pictured as sticks. All figures were prepared using Pymol.

However close inspection between the modelled parasite structure and human crystal structures shows that the human form possesses an added anti-parallel Beta sheet and elongated loop region which forms part of the active site (residues 192-214) at the C-terminal domain. The absence of this motif indicates that entirety of the active site has yet to be identified including the mode of binding for a potential inhibitor.

Preprints (www.preprints.org) | NOT PEER-REVIEWED | Posted: 17 October 2022 doi:10.20944/preprints202210.0220.v1

The discovery of new anthelmintic drug targets with broad-spectrum efficacy is expensive and time consuming. Currently, approximately $2.6 USD billion in direct costs and 10-15 years is the average length of time required to progress from the concept to a new marketable entity [40]. Our tertiary structure predictions and modelling analyses, with maybe the exclusion of glutamine synthetase, depict structures that have unique active site structures and in some cases, whole domains that can be used to take advantage of when considering unique differential drug targeting. The findings from our study can be incorporated in future investigations and may provide broad-spectrum efficacy particularly for all Clade III and V nematodes examined.

3. Materials and Methods

3.1. Animal Experiments and Collection of Parasite Material

The animal trial comprised of 20 animals, with 10 animals vaccinated twice with recombinant *Haemonchus* vaccine at 4-week interval and 10 animals served as control and received no treatment (Figure 1B). Two weeks after the second vaccination, all the animals were infected with 5,000 L3 *H. contortus*. Fecal egg counts were monitored twice weekly from day 16 post-infection until the end of the trial. Animals were bled and weighed weekly throughout the course of the trial. One control animal died because of an unrelated cause and therefore not included in sample collection or analysis. All 19 animals were killed 8 weeks post challenge and abomasa collected for adult worm counts. Each abomasum was cut open, washed and the 1/10 worms were collected for worm counts. Remaining worms were collected as described previously [9]. Briefly, abomasal contents were mixed 2:1 with 3% agar and the solidified agar blocks incubated at 37 °C in a saline bath. Adult male *H. contortus* worms were collected from the saline soon after emergence and stored in cryovials in liquid N_2 for subsequent DNA and RNA isolation.

3.2. Extraction of Nucleic Acids and Library Preparation

Male worms were only used for both DNA and RNA sequencing to account for any possible confounding factors associated with female-derived eggs or differences in sex ratio between samples. Pools of ten surviving *H. contortus* adult male worms from each animal were used for both DNA, amplicon and RNA sequencing. Prior to DNA extractions, *H. contortus* adult worms were washed with phosphate-buffered saline (PBS, pH 7.4) and incubated in an antibiotic solution (1 mg/ml ampicillin/1 mg/ml gentamicin) for 2 h to kill any surface-adherent bacteria [25, 28, 41]. The parasites were then washed twice with 2% sodium hypochlorite for 1 min each followed by five times with sterile PBS. Treated parasites were stored in PBS at -80 °C for downstream applications. High molecular weight genomic DNA for both WGS and amplicon sequencing was isolated from New Zealand anthelmintic-susceptible field strain *H. contortus* adult males, as previously described [13, 14, 23]. To account for any potential effects on the overall transcriptomes that may be induced with the sterilization techniques, *H. contortus* adult worms were only washed thoroughly with PBS as mentioned above for RNA extractions.

For amplicon sequencing, an alternative method was used as previously described for isolation of high molecular weight genomic DNA from rumen bacteria [42-44], and bacteria from uncooked meat samples [45-47]. Negative controls included to account for environmental contaminants present throughout the processing of the samples during the postmortem and lab environment consisted of 1 ml of PBS that was exposed to the equipment used, as well as the diluent Ultrapure water used for DNA extractions. The specificity of genomic DNA was verified by automated Sanger sequencing of the second internal transcribed spacer (ITS-2) of nuclear ribosomal DNA following PCR amplification from genomic DNA. Total DNA concentrations were determined using a NanoDrop® ND-1000 (Thermo Scientific Inc.) and a Qubit Fluorometer dsDNA BR Kit (Invitrogen), in accordance with the manufacturer's instructions. Genomic DNA integrity was verified by agarose gel electrophoresis and using a 2000 BioAnalyzer (Agilent). Libraries were prepared using the NEBNext® DNA preparation kit prior to sequencing with the HiSeq 2500

Preprints (www.preprints.org) | NOT PEER-REVIEWED | Posted: 17 October 2022 doi:10.20944/preprints202210.0220.v1

platform with v3 chemistry, and via single step PCR prior to sequencing using the Illumina MiSeq Nano 500 cycle Kit_V1 chemistry, for WGS and 16*S* (V3-V4 rRNA) metagenomic amplicon sequencing, respectively.

RNA from snap-frozen samples containing 100 µl of packed worms were lysed using an 18V drill loaded with a disposable RNAase-free polypropylene Micro-Pestle (Qiagen) until the mix is ground to a fine white powder. To the ground sample 250 µl of pre-warmed (40°C) TRizol (Thermo Scientific Inc.) was added and mixed thoroughly according to the manufacturer's instructions, snap-frozen in liquid N_2 and the homogenization of snap frozen samples in TRizol was repeated for five rounds in total to ensure complete disruption of the sample. To the homogenized sample, 750 µl of pre-warmed TRizol and 0.1 volume of chloroform were added, thoroughly mixed and centrifuged at 20,000 × *g* for 10 min at 4°C. The upper aqueous phase was transferred into a new Eppendorf tube and an equal volume of isopropanol and 0.1 volume of 3 M sodium acetate (pH 5.5) were added and gently mixed, and the mixture was stored at -20°C overnight. The RNA pellets were precipitated with ethanol, re-suspended in nuclease-free water (Life Technologies) and DNase I treated. RNA yield and quality were assessed using the Bioanalyzer 2100 with the RNA 6000 Nano assay reagent kit from Agilent (Santa Clara, CA) and stored at -80°C. Libraries were prepared using the Illumina TruSeq RNA preparation kit and rRNA was removed using the Ribo-Zero kit prior to sequencing with the HiSeq 2500 platform with v3 chemistry.

3.3. DNA and RNA-Seq Raw Reads Pre-processing

The whole genome shotgun sequencing and transcriptomics reads were evaluated using FastQC v0.11.8 [48]. The reads were then trimmed for Illumina adapter sequences and low quality (below Q30) regions using Trimmomatic v0.39 [49].

3.4. Whole Genome Sequencing and Identification of SNP Variants

To explore the levels of genetic diversity at the whole genome level, sites of genetic variation or single nucleotide polymorphisms (SNPs) between treated and control groups were identified by investigating two *H. contortus* genomic DNA samples extracted from pooled treatment (*n*=10) and non-treated (*n*=9) groups. Genomics services were provided by Novogene including library preparation, QC and sequencing using the Illumina HiSeq™ PE150 to generate 50Gb raw data for each sample. For the WGS analysis, the "mem" algorithm of BWA v0.7.17-r1188 [PM3] was used to map the DNA whole genome shotgun sequencing reads against the *H. contortus* NZ_HCO_NP v1.0 genome [13, 14, 23] with default settings. The "view" function Samtools v1.9 [50], the "call" function of bcftools v1.9 [51], was used to call SNPs with the consensus caller parameter specified and only variant sites returned. The resulting variants were filtered to only include bi-allelic SNPs with a score of 100 or more. The filtered SNPs were converted to values of 1 when not homozygous with the reference allele. Kilobases on the NZ_HCO_NP genome with at least 99 differential variants between the control and vaccinated samples were evaluated a Fisher's exact test in R v4.0.2 [52]. The histograms of filtered SNPs per kilobase were printed using ggplot2 v3.3.3 [53], with a bandwidth of 10-Kbp for the chromosomes and 100 bp for the *H. contortus* NZ_HCO_NP mitochondrial genome [14, 23, 24, 54].

3.5.16. S rRNA Gene Library Preparation, MiSeq Sequencing and Microbiome Profiling

To investigate the impact of vaccine treatment on the parasite microbiota, adult male *H. contortus* populations from sheep treated with our recombinant vaccine (*n*=10) with worms from non-treated control animals (*n*=9). High molecular weight genomic DNA was extracted from samples for metagenomic 16S Amplicon Sequencing of the V3-V4 hypervariable region as previously described [55, 56]. The prepared DNA samples had at least 50 ng of purified gDNA for each sample at a concentration of at least 10 ng/µl with the majority of DNA greater than 10 Kb in size and with minimal lower molecular weight smearing or RNA contamination.

 doi:10.20944/preprints202210.0220.v1

The V3-V4 hypervariable region within the 16S rRNA gene of approximately 500 bp was amplified using a set of commonly used primers (Table S1). The 19 libraries were prepared using the Illumina 16S V3-V4 rRNA library preparation method by the Massey Genome Service (Palmerston North, New Zealand) using their dual index PCR primers which flank the V3-V4 hyper-variable region of 16S rRNA, using a single step PCR library preparation method. The libraries were pooled by equal molarity before loading onto one Illumina MiSeq™ 2× 250 base PE Nano run, version 2 chemistry to generate one million paired-end reads.

The processing of the amplicon reads followed a modified version of the pipeline described in [57]. The reads produced by the sequencing instrument were paired using the program FLASH2 [58]. Paired reads were then quality trimmed using Trimmomatic v0.38 [49]. The trimmed reads were reformatted as Fasta, and the read headers were modified to include the sample name. All reads were compiled into a single file, and Mothur (24) was used to remove reads with homopolymers longer than 10 nt and to collapse the reads into unique representatives. The collapsed reads were clustered using Swarm [59]. The clustered reads were filtered based on their abundance, keeping representatives that were a) present in one sample with a relative abundance >0.1%, b) present in >2% of the samples with a relative abundance >0.01% or c) present in 5% of the samples at any abundance level. The selected representatives were annotated using Qiime [60] with the Silva database v138 [61]. The annotated tables were then used for downstream statistical analysis.

3.6. Transcriptome Sequencing, Assembly, Functional Annotation and Differential Expression Analysis

We investigated the genetic mechanisms involved in vaccine escape or evasion and whether there is a vaccine-induced immunity effect that influences gene expression levels. For this work, total RNA was extracted using the attached protocol also from adult male *H. contortus* populations from sheep treated (n=10) and non-treated control animals (n=9). RNA samples were all prepared to the recommended specifications for sequencing, i.e. >2ug of RNA at >50ng/ul, OD260/280>2.0 and no degradation or DNA contamination. Transcriptomics services were provided by Novogene including: lncRNA-Seq (including rRNA removal (Ribo Zero) and strand specific library preparation/sequencing/data QC, Illumina PE150, to provide 15Gb raw data per sample (Table S2).

For the transcriptome analysis, RNA-seq reads were mapped against the *H. contortus* NZ_HCO_NP v1.0 genome [13, 14, 23] using the spliced mapper STAR v2.7.1a [62]. Genes were called from the resulting sorted BAM files with cufflinks v2.2.1 [63] with the "fr-secondstrand" library type option given. The resulting genes were visualised using IGV v2.4.9 [64]. The reads were assigned to cufflinks-derived genes using the "featurecounts" function of the subread package v1.5.0-p3 [65] with the "-p" and "-s 2" parameters set to count reversely-stranded pairs. The counts were compiled and tabulated and differential expression was done using the DESeq2 package v1.30.2 [66] with default parameters in R v4.0.2 [52].

Possible protein coding regions within the assembled transcripts were identified using the TransDecoder program v5.5.0 implemented in the Trinity software distribution v2.8.5 [67]. The protein coding regions were searched against the NCBI NR protein sequence database using the blastp function of diamond v2.0.6 [68] with the output format of XML specified. The results were imported into OmicsBox v1.4.11 (https://www.biobam.com) where the BLAST2GO and annotation functions [69] were used with default settings. InterProScan v5.50-84.0 [70] and eggNOG-Mapper v1.0.3 with EggNOG v5.0.0 [71] were further used with default settings to annotate the predicted proteins. Gene ontology terms were assigned to each gene (Table S3), and enrichment analysis was performed using agriGO v2. 0 [72] to evaluate the significance of each gene ontology category. Five target DEG sequences; astacin *astl*, carbonate dehydratase *ca2*, phospholipase

 doi:10.20944/preprints202210.0220.v1

pla2, glutamine synthetase *glul* and fatty acid-binding protein 3 *fabp3*, were selected for downstream analysis of gene family evolution and protein modelling.

3.7. Gene Family Evolution

The five target DEG protein sequences common for both hosts were searched against the Wormbase Parasite [73] protein BLAST database using the BLASTP v2.9.0+ [74] search with default settings as previously described [75]. Proteomes containing hits with over 70% identity, scores at least 50% of the *H. contortus* NZ_HCO_NP field strain v1.0 genome match and hit sequence lengths at least 75% of the query sequence lengths were downloaded from WormBase. We gathered predicted proteomes of selected Nematoda representing Clades III, V, IV, C, I, Platyhelminthes belonging to Clades Monogenea, Trematoda, Cestoda, Rhabditophora, with *Homo sapiens*, *Mus musculus* and *Danio rerio* as outgroups. To determine homologs of the five target *H. contortus* DEGs, we identified single-copy orthologous groups (OGs) in the five proteomes using OrthoFinder v 2.5.2 [76], with cluster selection based on at least 75% species present with a single protein in each cluster. The extracted proteins were subjected to phylogenetic analysis with 1,000 bootstrap replicates with maximum likelihood (ML) inferences for each resulting trimmed gene-cluster generated to infer the species tree under a multiple-species coalescent model. An evolutionary model was selected automatically for each cluster and visualized in Geneious Prime v2019.1.3 [77].

3.8. Protein Modelling and Structural Analysis

The Position-Specific Iterative Basic Local Alignment Search Tool (PSI-BLAST) [78] was used to compare the protein sequences associated with the DEGs of interest with the corresponding deposited structures in the Protein Data Bank (PDB). Structural models of a subset of candidate parasite vaccine targets were generated utilizing the ICM-Homology modeling algorithm and refinement tools [79-81] available in the ICM-Pro modelling suite (Molsoft LLC; molsoft.com). ICM-Pro was also used for template searches for our candidate proteins, allowing for automated alignment and inspection before prior to modelling the target protein. The modelled enzymes are detailed in Supplementary Table S4. The active site residues were deduced and visualized using PyMOL Molecular Graphics System v2.0 [82] where the model was superimposed with their parent structures co-crystallized with substrate or inhibitor.

Supplementary Materials: The following supporting information can be downloaded at: www.mdpi.com/xxx/s1, Figure S1: Statistics and sample grouping of *H. contortus* adult males exposed to the vaccine response or the control group de novo transcriptome assemblies. Raw counts (A) were normalized (B) by variance stabilizing transformation (D) and profiles are outlined using principal component analyses (PCA) of normalized transcript counts measured in worms collected from vaccinated or control sheep (C). Volcano plot of significantly differentially expressed (DE) genes determined using DESeq2 (E); Table S1: List of primer sequences used for 16S amplicon sequencing of the V3-V4 hypervariable region; Table S2: List of top *H. contortus* differentially expressed protein coding genes and long non-coding RNAs; Table S3: Top GO classifications of significantly differentially expressed genes (DEGs) in *H. contortus* recovered from vaccinated and control sheep; Table S4: List of top *H. contortus* differentially expressed (DE) protein coding genes selected for protein modelling and structural analysis.

Author Contributions: N.P. and S.U. conceived the project and acquired the funding. N.P. and S.U. with assistance from Parasitology team members performed sample collection and acquired parasite material. N.P. processed all samples from experiments, analyzed and interpreted the data, and wrote the manuscript. P.H.M. and R.J. provided statistical support and guidance with bioinformatics analysis. V.C. performed the protein modelling analysis and interpretation of the results. All authors have read and agreed to the published version of the manuscript.

Funding: This study was supported by the AgResearch Ltd. Strategic Science Investment Fund (SSIF), contract number A25605 to N.P and S.U. This work was also supported in part by the Agricultural and Marketing Research and Development Trust (AGMARDT) Postdoctoral Fellowship Programme, Grant P17001 to N.P and Grant P14003 to S.U.

Institutional Review Board Statement: The animal study was reviewed and approved by the AgResearch Grasslands Animal Ethics Committee, Palmerston North, New Zealand (AEC application number 14628). Written informed consent was obtained from the owners for the participation of their animals in this study.

Informed Consent Statement: Not applicable.
Data Availability Statement: All data generated during this study are included in this published article and its supplementary information files. Raw sequence reads were submitted to NCBI Sequence Read Archive (SRA) and are available under BioProject accession PRJNA517503 (runs SRR14054466-SRR14054505).

Acknowledgments: We thank Ron Ronimus and Charles Hefer for their critical revisions and comments on the manuscript.

Conflicts of Interest: The authors declare no conflict of interest.

References

1. Besier, R.; Kahn, L.; Sargison, N.; Van Wyk, J., Diagnosis, treatment and management of *Haemonchus contortus* in small ruminants. In *Advances in Parasitology*, Elsevier: 2016; Vol. 93, pp 181-238.
2. Kaplan, R. M.; Vidyashankar, A. N., An inconvenient truth: global worming and anthelmintic resistance. *Veterinary parasitology* **2012,** *186*, 70-78.
3. Palevich, N.; Maclean, P. H.; Candy, P. M.; Taylor, W.; Mladineo, I.; Cao, M., Untargeted Multimodal Metabolomics Investigation of the *Haemonchus contortus* Exsheathment Secretome. *Cells* **2022,** *11*, 2525.
4. Geary, T. G.; Sakanari, J. A.; Caffrey, C. R., Anthelmintic drug discovery: into the future. *J Parasitol* **2015,** *101*, 125-133.
5. Bassetto, C.; Amarante, A., Vaccination of sheep and cattle against haemonchosis. *Journal of helminthology* **2015,** *89*, 517.
6. Umair, S.; Bouchet, C.; Palevich, N.; Simpson, H., *Teladorsagia circumcincta* 1,6-Bisphosphate Aldolase: Molecular and Biochemical Characterisation, Structure Analysis and Recognition by Immune Hosts. *Parasitologia* **2021,** *1*.
7. Umair, S.; Bouchet, C.; Palevich, N.; Simpson, H. V., Characterisation and structural analysis of glyoxylate cycle enzymes of *Teladorsagia circumcincta*. *Molecular and Biochemical Parasitology* **2020,** *240*, 111335.
8. Umair, S.; Bouchet, C. L. G.; Deng, Q.; Palevich, N.; Simpson, H. V., Characterisation of a *Teladorsagia circumcincta* glutathione transferase. *Molecular and Biochemical Parasitology* **2020,** *239*, 111316.
9. Umair, S.; Knight, J. S.; Bland, R. J.; Simpson, H. V., Molecular and biochemical characterisation of arginine kinases in *Haemonchus contortus* and *Teladorsagia circumcincta*. *Experimental Parasitology* **2013,** *134*, 362-367.
10. Sallé, G.; Laing, R.; Cotton, J. A.; Maitland, K.; Martinelli, A.; Holroyd, N.; Tracey, A.; Berriman, M.; Smith, W. D.; Newlands, G. F., Transcriptomic profiling of nematode parasites surviving vaccine exposure. *International journal for parasitology* **2018,** *48*, 395-402.
11. Kennedy, D. A.; Read, A. F., Why does drug resistance readily evolve but vaccine resistance does not? *Proceedings of the Royal Society B: Biological Sciences* **2017,** *284*, 20162562.
12. Brueggemann, A. B.; Pai, R.; Crook, D. W.; Beall, B., Vaccine escape recombinants emerge after pneumococcal vaccination in the United States. *PLoS Pathog* **2007,** *3*, e168.
13. Palevich, N.; Maclean, P. H.; Baten, A.; Scott, R. W.; Leathwick, D. M., The Genome Sequence of the Anthelmintic-Susceptible New Zealand *Haemonchus contortus*. *Genome biology and evolution* **2019,** *11*, 1965-1970.
14. Palevich, N.; Maclean, P.; Baten, A.; Scott, R.; Leathwick, D. M., The complete mitochondrial genome of the New Zealand parasitic roundworm *Haemonchus contortus* (Trichostrongyloidea: Haemonchidae) field strain NZ_Hco_NP. *Mitochondrial DNA Part B* **2019,** *4*, 2208-2210.
15. Sinnathamby, G.; Henderson, G.; Umair, S.; Janssen, P.; Bland, R.; Simpson, H., The bacterial community associated with the sheep gastrointestinal nematode parasite *Haemonchus contortus*. *PLoS ONE* **2018,** *13*.
16. Jourdan, P. M.; Lamberton, P. H.; Fenwick, A.; Addiss, D. G., Soil-transmitted helminth infections. *The Lancet* **2018,** *391*, 252-265.
17. Charlier, J.; van der Voort, M.; Kenyon, F.; Skuce, P.; Vercruysse, J., Chasing helminths and their economic impact on farmed ruminants. *Trends in parasitology* **2014,** *30*, 361-367.
18. Gibbons, L. M., Revision of the genus Haemonchus Cobb, 1898 (Nematoda: Trichostrongylidae). *Systematic parasitology* **1979,** *1*, 3-24.
19. Lichtenfels, J. R.; Pilitt, P.; Hoberg, E. P., New morphological characters for identifying individual specimens of Haemonchus spp.(Nematoda: Trichostrongyloidea) and a key to species in ruminants of North America. *The Journal of parasitology* **1994**, 107-119.
20. Bisset, S.; Knight, J.; Bouchet, C., A multiplex PCR-based method to identify strongylid parasite larvae recovered from ovine faecal cultures and/or pasture samples. *Veterinary parasitology* **2014,** *200*, 117-127.
21. Amarante, M.; Santos, M.; Bassetto, C.; Amarante, A., PCR primers for straightforward differentiation of Haemonchus contortus, Haemonchus placei and their hybrids. *Journal of helminthology* **2017**, 757-761.

22. Palevich, N.; Britton, C.; Kamenetzky, L.; Mitreva, M.; de Moraes Mourão, M.; Bennuru, S.; Quack, T.; Scholte, L. L. S.; Tyagi, R., Tackling hypotheticals in helminth genomes. *Trends in parasitology* **2018,** *34*, 179-183.
23. Palevich, N.; Maclean, P. H.; Choi, Y.-J.; Mitreva, M., Characterization of the Complete Mitochondrial Genomes of Two Sibling Species of Parasitic Roundworms, *Haemonchus contortus* and *Teladorsagia circumcincta*. *Frontiers in Genetics* **2020,** *11*.
24. Palevich, N.; Maclean, P. H.; Mitreva, M.; Scott, R.; Leathwick, D., The complete mitochondrial genome of the New Zealand parasitic roundworm *Teladorsagia circumcincta* (Trichostrongyloidea: Haemonchidae) field strain NZ_Teci_NP. *Mitochondrial DNA Part B* **2019,** *4*, 2869-2871.
25. El-Ashram, S.; Suo, X., Exploring the microbial community (microflora) associated with ovine Haemonchus contortus (macroflora) field strains. *Scientific reports* **2017,** *7*, 1-13.
26. Midha, A.; Schlosser, J.; Hartmann, S., Reciprocal Interactions between Nematodes and Their Microbial Environments. *Frontiers in Cellular and Infection Microbiology* **2017,** *7*.
27. Mafuna, T.; Soma, P.; Tsotetsi-Khambule, A.; Hefer, C.; Muchadeyi, F.; Thekisoe, O.; Pierneef, R., Bacterial profiling of Haemonchus contortus gut microbiome infecting Dohne Merino sheep in South Africa. *Scientific reports* **2021,** *11*, 1-11.
28. Hogan, G.; Walker, S.; Turnbull, F.; Curiao, T.; Morrison, A. A.; Flores, Y.; Andrews, L.; Claesson, M. J.; Tangney, M.; Bartley, D. J., Microbiome analysis as a platform R&D tool for parasitic nematode disease management. *The ISME journal* **2019,** *13*, 2664-2680.
29. Oh, C.-S.; Toke, D. A.; Mandala, S.; Martin, C. E., ELO2 and ELO3, Homologues of the *Saccharomyces cerevisiae* ELO1 Gene, Function in Fatty Acid Elongation and Are Required for Sphingolipid Formation. *Journal of Biological Chemistry* **1997,** *272*, 17376-17384.
30. Garcia-Arranz, M.; Maldonado, A. M.; Mazon, M. J.; Portillo, F., Transcriptional control of yeast plasma membrane H (+)-ATPase by glucose. Cloning and characterization of a new gene involved in this regulation. *Journal of Biological Chemistry* **1994,** *269*, 18076-18082.
31. Zhang, X.; Wang, W.; Zhu, W.; Dong, J.; Cheng, Y.; Yin, Z.; Shen, F., Mechanisms and Functions of Long Non-Coding RNAs at Multiple Regulatory Levels. *International journal of molecular sciences* **2019,** *20*, 5573.
32. Sun, L.; Li, D.; Yuan, Y.; Wang, D., Intestinal long non-coding RNAs in response to simulated microgravity stress in *Caenorhabditis elegans*. *Scientific Reports* **2021,** *11*, 1997.
33. Ma, G.; Wang, T.; Korhonen, P. K.; Stroehlein, A. J.; Young, N. D.; Gasser, R. B., Dauer signalling pathway model for Haemonchus contortus. *Parasites & Vectors* **2019,** *12*, 187.
34. Duque-Correa, M. A.; Maizels, R. M.; Grencis, R. K.; Berriman, M., Organoids - New Models for Host-Helminth Interactions. *Trends in Parasitology* **2020,** *36*, 170-181.
35. Consortium, I. H. G., Comparative genomics of the major parasitic worms. *Nature genetics* **2019,** *51*, 163.
36. Ruskamo, S.; Nieminen, T.; Kristiansen, C. K.; Vatne, G. H.; Baumann, A.; Hallin, E. I.; Raasakka, A.; Joensuu, P.; Bergmann, U.; Vattulainen, I., Molecular mechanisms of Charcot-Marie-Tooth neuropathy linked to mutations in human myelin protein P2. *Scientific reports* **2017,** *7*, 1-13.
37. Chen, H.; Knerr, L.; Åkerud, T.; Hallberg, K.; Öster, L.; Rohman, M.; Österlund, K.; Beisel, H.-G.; Olsson, T.; Brengdhal, J., Discovery of a novel pyrazole series of group X secreted phospholipase A2 inhibitor (sPLA2X) via fragment based virtual screening. *Bioorganic & medicinal chemistry letters* **2014,** *24*, 5251-5255.
38. Okada, A.; Sano, K.; Nagata, K.; Yasumasu, S.; Ohtsuka, J.; Yamamura, A.; Kubota, K.; Iuchi, I.; Tanokura, M., Crystal structure of zebrafish hatching enzyme 1 from the zebrafish Danio rerio. *Journal of molecular biology* **2010,** *402*, 865-878.
39. Krajewski, W. W.; Collins, R.; Holmberg-Schiavone, L.; Jones, T. A.; Karlberg, T.; Mowbray, S. L., Crystal structures of mammalian glutamine synthetases illustrate substrate-induced conformational changes and provide opportunities for drug and herbicide design. *Journal of molecular biology* **2008,** *375*, 217-228.
40. Tamimi, N. A.; Ellis, P., Drug development: from concept to marketing! *Nephron Clinical Practice* **2009,** *113*, c125-c131.
41. Dirksen, P.; Marsh, S. A.; Braker, I.; Heitland, N.; Wagner, S.; Nakad, R.; Mader, S.; Petersen, C.; Kowallik, V.; Rosenstiel, P., The native microbiome of the nematode Caenorhabditis elegans: gateway to a new host-microbiome model. *BMC biology* **2016,** *14*, 1-16.
42. Palevich, N.; Kelly, W. J.; Leahy, S. C.; Altermann, E.; Rakonjac, J.; Attwood, G. T., The complete genome sequence of the rumen bacterium *Butyrivibrio hungatei* MB2003. *Standards in Genomic Sciences* **2017,** *12*, 72.
43. Palevich, N.; Kelly, W. J.; Leahy, S. C.; Denman, S.; Altermann, E.; Rakonjac, J.; Attwood, G. T., Comparative genomics of rumen *Butyrivibrio* spp. uncovers a continuum of polysaccharide-degrading capabilities. *Applied and environmental microbiology* **2019,** *86*.
44. Palevich, N.; Maclean, P. H.; Kelly, W. J.; Leahy, S. C.; Rakonjac, J.; Attwood, G. T., Complete Genome Sequence of the Polysaccharide-Degrading Rumen Bacterium *Pseudobutyrivibrio xylanivorans* MA3014 Reveals an Incomplete Glycolytic Pathway. *Genome Biology and Evolution* **2020,** *12*, 1566-1572.
45. Palevich, N.; Palevich, F. P.; Maclean, P. H.; Altermann, E.; Gardner, A.; Burgess, S.; Mills, J.; Brightwell, G., Comparative genomics of Clostridium species associated with vacuum-packed meat spoilage. *Food Microbiology* **2021,** *95*, 103687.
46. Burgess, S. A.; Palevich, F. P.; Gardner, A.; Mills, J.; Brightwell, G.; Palevich, N., Occurrence of genes encoding spore germination in *Clostridium* species that cause meat spoilage. *Microbial Genomics* **2022,** *8*.

47. Palevich, N.; Palevich, F. P.; Gardner, A.; Brightwell, G.; Mills, J., Genome collection of *Shewanella* spp. isolated from spoiled lamb. *Frontiers in Microbiology* **2022,** *13*.
48. Andrews, S., FastQC: a quality control tool for high throughput sequence data. In Babraham Bioinformatics, Babraham Institute, Cambridge, United Kingdom: 2010.
49. Bolger, A. M.; Lohse, M.; Usadel, B., Trimmomatic: a flexible trimmer for Illumina sequence data. *Bioinformatics* **2014,** *30*, 2114-2120.
50. Li, H.; Handsaker, B.; Wysoker, A.; Fennell, T.; Ruan, J.; Homer, N.; Marth, G.; Abecasis, G.; Durbin, R., The sequence alignment/map format and SAMtools. *Bioinformatics* **2009,** *25*, 2078-2079.
51. Li, H., A statistical framework for SNP calling, mutation discovery, association mapping and population genetical parameter estimation from sequencing data. *Bioinformatics* **2011,** *27*, 2987-2993.
52. R Core Team *R: A language and environment for statistical computing*, R Foundation for Statistical Computing: Vienna, Austria, 2015.
53. Wickham, H., ggplot2. Wiley Interdisciplinary Reviews: Computational Statistics **2011,** 3, 180-185.
54. Palevich, N.; Maclean, P. H., Sequencing and reconstructing helminth mitochondrial genomes directly from genomic next-generation sequencing data. In *Parasite Genomics: Methods and Protocols*, de Pablos, L. M.; Sotillo, J., Eds. Humana Press: New York, 2021.
55. Palevich, N.; Maclean, P. H.; Carvalho, L.; Jauregui, R., 16S rRNA Gene Amplicon Profiling of the New Zealand parasitic blowfly *Calliphora vicina*. *Microbiology Resource Announcements* **2021,** *10*, e00289-00221.
56. Palevich, N.; Maclean, P. H.; Carvalho, L.; Jauregui, R., Bacterial diversity profiling of the New Zealand parasitic blowfly *Lucilia sericata* based on 16S rRNA gene amplicon sequencing. *Microbiology Resource Announcements* **2021,** *10*, e00257-00221.
57. Kozich, J. J.; Westcott, S. L.; Baxter, N. T.; Highlander, S. K.; Schloss, P. D., Development of a dual-index sequencing strategy and curation pipeline for analyzing amplicon sequence data on the MiSeq Illumina sequencing platform. *Applied and environmental microbiology* **2013,** *79*, 5112-5120.
58. Magoč, T.; Salzberg, S. L., FLASH: fast length adjustment of short reads to improve genome assemblies. *Bioinformatics* **2011,** *27*, 2957-2963.
59. Mahé, F.; Rognes, T.; Quince, C.; de Vargas, C.; Dunthorn, M., Swarm: robust and fast clustering method for amplicon-based studies. *PeerJ* **2014,** *2*, e593.
60. Caporaso, J. G.; Kuczynski, J.; Stombaugh, J.; Bittinger, K.; Bushman, F. D.; Costello, E. K.; Fierer, N.; Pena, A. G.; Goodrich, J. K.; Gordon, J. I., QIIME allows analysis of high-throughput community sequencing data. *Nature methods* **2010,** *7*, 335-336.
61. Quast, C.; Pruesse, E.; Yilmaz, P.; Gerken, J.; Schweer, T.; Yarza, P.; Peplies, J.; Glöckner, F. O., The SILVA ribosomal RNA gene database project: improved data processing and web-based tools. *Nucleic acids research* **2012,** *41*, D590-D596.
62. Dobin, A.; Davis, C. A.; Schlesinger, F.; Drenkow, J.; Zaleski, C.; Jha, S.; Batut, P.; Chaisson, M.; Gingeras, T. R., STAR: ultrafast universal RNA-seq aligner. *Bioinformatics* **2013,** *29*, 15-21.
63. Trapnell, C.; Roberts, A.; Goff, L.; Pertea, G.; Kim, D.; Kelley, D. R.; Pimentel, H.; Salzberg, S. L.; Rinn, J. L.; Pachter, L., Differential gene and transcript expression analysis of RNA-seq experiments with TopHat and Cufflinks. *Nature protocols* **2012,** *7*, 562.
64. Robinson, J. T.; Thorvaldsdóttir, H.; Winckler, W.; Guttman, M.; Lander, E. S.; Getz, G.; Mesirov, J. P., Integrative genomics viewer. *Nature biotechnology* **2011,** *29*, 24-26.
65. Liao, Y.; Smyth, G. K.; Shi, W., The Subread aligner: fast, accurate and scalable read mapping by seed-and-vote. *Nucleic acids research* **2013,** *41*, e108-e108.
66. Love, M. I.; Huber, W.; Anders, S., Moderated estimation of fold change and dispersion for RNA-seq data with DESeq2. *Genome biology* **2014,** *15*, 1-21.
67. Grabherr, M. G.; Haas, B. J.; Yassour, M.; Levin, J. Z.; Thompson, D. A.; Amit, I.; Adiconis, X.; Fan, L.; Raychowdhury, R.; Zeng, Q., Trinity: reconstructing a full-length transcriptome without a genome from RNA-Seq data. *Nature biotechnology* **2011,** *29*, 644.
68. Buchfink, B.; Xie, C.; Huson, D. H., Fast and sensitive protein alignment using DIAMOND. *Nature Methods* **2015,** *12*, 59.
69. Conesa, A.; Götz, S.; García-Gómez, J. M.; Terol, J.; Talón, M.; Robles, M., Blast2GO: a universal tool for annotation, visualization and analysis in functional genomics research. *Bioinformatics* **2005,** *21*, 3674-3676.
70. Jones, P.; Binns, D.; Chang, H.-Y.; Fraser, M.; Li, W.; McAnulla, C.; McWilliam, H.; Maslen, J.; Mitchell, A.; Nuka, G., InterProScan 5: genome-scale protein function classification. *Bioinformatics* **2014,** *30*, 1236-1240.
71. Huerta-Cepas, J.; Szklarczyk, D.; Heller, D.; Hernández-Plaza, A.; Forslund, S. K.; Cook, H.; Mende, D. R.; Letunic, I.; Rattei, T.; Jensen, L. J., eggNOG 5.0: a hierarchical, functionally and phylogenetically annotated orthology resource based on 5090 organisms and 2502 viruses. *Nucleic acids research* **2019,** *47*, D309-D314.
72. Tian, T.; Liu, Y.; Yan, H.; You, Q.; Yi, X.; Du, Z.; Xu, W.; Su, Z., agriGO v2. 0: a GO analysis toolkit for the agricultural community, 2017 update. *Nucleic acids research* **2017,** *45*, W122-W129.
73. Howe, K. L.; Bolt, B. J.; Shafie, M.; Kersey, P.; Berriman, M., WormBase ParaSite− a comprehensive resource for helminth genomics. *Molecular and biochemical parasitology* **2017,** *215*, 2-10.
74. Camacho, C.; Coulouris, G.; Avagyan, V.; Ma, N.; Papadopoulos, J.; Bealer, K.; Madden, T. L., BLAST+: architecture and applications. *BMC bioinformatics* **2009,** *10*, 1-9.

75. Trumbić, Ž.; Hrabar, J.; Palevich, N.; Carbone, V.; Mladineo, I., Good host - bad host: molecular and evolutionary basis for survival, its failure, and virulence factors of the zoonotic nematode Anisakis pegreffii. In Cold Spring Harbor Laboratory: 2021.
76. Emms, D. M.; Kelly, S., OrthoFinder: solving fundamental biases in whole genome comparisons dramatically improves orthogroup inference accuracy. *Genome biology* **2015,** *16*, 1-14.
77. Kearse, M.; Moir, R.; Wilson, A.; Stones-Havas, S.; Cheung, M.; Sturrock, S.; Buxton, S.; Cooper, A.; Markowitz, S.; Duran, C., Geneious Basic: an integrated and extendable desktop software platform for the organization and analysis of sequence data. *Bioinformatics* **2012,** *28*, 1647-1649.
78. Altschul, S. F.; Madden, T. L.; Schäffer, A. A.; Zhang, J.; Zhang, Z.; Miller, W.; Lipman, D. J., Gapped BLAST and PSI-BLAST: a new generation of protein database search programs. *Nucleic Acids Research* **1997,** *25*, 3389-3402.
79. Abagyan, R.; Totrov, M.; Kuznetsov, D., ICM-A new method for protein modeling and design: Applications to docking and structure prediction from the distorted native conformation. *Journal of computational chemistry* **1994,** *15*, 488-506.
80. Abagyan, R.; Batalov, S.; Cardozo, T.; Totrov, M.; Webber, J.; Zhou, Y., Homology modeling with internal coordinate mechanics: deformation zone mapping and improvements of models via conformational search. *Proteins: Structure, Function, and Bioinformatics* **1997,** *29*, 29-37.
81. Cardozo, T.; Totrov, M.; Abagyan, R., Homology modeling by the ICM method. *Proteins: Structure, Function, and Bioinformatics* **1995,** *23*, 403-414.
82. Schrodinger, L., The PyMOL molecular graphics system. *Version* **2010,** *2.0*, 0.